Hindawi Publishing Corporation
Mathematical Problems in Engineering
Volume 2016, Article ID 2879524, 10 pages
http://dx.doi.org/10.1155/2016/2879524

Research Article

Time Irreversibility from Time Series for Analyzing Oil-in-Water Flow Transition

Du Meng,[1] Chen Xiao-yan,[1] Liu Hong-ying,[1] He Qing,[1] Bai Rui-xiang,[1] Liu Weixin,[2] and Li Zewei[2]

[1]*College of Electronic Information and Automation, Tianjin University of Science and Technology, Tianjin 300222, China*
[2]*School of Computer Science & Software Engineering, Tianjin Polytechnic University, Tianjin 300387, China*

Correspondence should be addressed to Du Meng; mdu@tust.edu.cn

Received 31 December 2015; Revised 20 February 2016; Accepted 7 March 2016

Academic Editor: Konstantinos Karamanos

We first experimentally collect conductance fluctuation signals of oil-in-water two-phase flow in a vertical pipe. Then we detect the flow pattern asymmetry character from the collected signals with multidimensional time irreversibility and multiscale time irreversibility index. Moreover, we propose a novel criterion, that is, AMSI (average of multiscale time irreversibility), to quantitatively investigate the oil-in-water two-phase flow pattern dynamics. The results show that AMSI is sensitive to the flow pattern evolution that can be used to predict the flow pattern transition and bubble coalescence.

1. Introduction

Oil-in-water two-phase flow widely exists in petroleum industry such as crude oil production and transportation. Due to the existence of fluid turbulence and phase interfacial interaction, the mixed fluid often exhibits complex behaviors. In particular, under very low mixture velocity, the existence of bubble coalescence phenomenon leads to more complex fluid dynamics. In this regard, characterizing the oil-in-water two-phase flow structure and dynamics is still quite a challenging problem which is helpful for the flow parameters measurement and pipe pressure drop prediction.

Study on oil-in-water two-phase flow dates back to the 1960s, and early researchers' main focus is on the flow pattern observation and definition. Govier et al. [1] first define the dispersed oil phase in 1.04-inch inner diameter pipe as oil bubble and slug. Then Flores et al. [2] redefine the dispersed oil phase as three different flow patterns, that is, slug flow, bubble flow, and dispersed bubble. This definition for dispersed oil phase is more elaborate that has been approved by several researchers [3, 4]. Recently, researchers are more concerned about oil-in-water two-phase flow under certain flow conditions, such as two-phase flow in bend pipe [5], two-phase flow in microchannels [6], and high-viscosity oil-water two-phase flow [7]. In addition, more advanced experimental methods are adopted to explore the oil bubble characteristics. The methods such as miniprobe detection [8], high speed photography [9], microwave measurement [10], process tomography [11], and PIV technology [12] have been applied to study the characteristics of oil-in-water two-phase flow.

In recent years, characterizing complex systems from time series has attracted much attention [13, 14]. These signals are time series that are collected to reflect the conductance or pressure fluctuations of the mixed fluid. Note that adopting different signal processing methods would reveal different aspects of flow characteristics. For example, time-frequency method [15] focuses on revealing the motion behaviors of dispersed phase, wavelet analysis [16] and Hilbert-Huang transform method [17] mainly reflect the multiscale and polymorphism dynamics, and nonlinear information analysis techniques [18] are advanced in complex fluid dynamic indication. It is worth noting that complex network has been proved to be an effective tool to characterize the system dynamics [19–21], and the fluid dynamic can also be revealed with mapping the fluctuating signals to networks [22–26].

In general, the flow dynamics revealed from experiment fluctuation signals are less affected by flow condition such as flow rate, pipe diameter, and pipe direction; these methods have attracted many researchers' attention in recent years.

It is a remarkable fact that under low mixture velocity the oil-in-water two-phase flow exhibits quite complex dynamics. First, the fluid exhibits spatial asymmetry structure due to the bubble coalescence. How to characterize this fluid asymmetry is still a difficult problem. In addition, how to effectively characterize the flow pattern transition phenomenon, for example, from slug flow to bubble flow, is still unsolved. Therefore, developing a reliable tool to characterize the oil-in-water two-phase flow dynamics and flow pattern evolution character is quite a necessary issue. Recently, time irreversibility index has been proved to be a powerful tool to detect system dynamics and quantify the existence of system disequilibrium [27]. If the statistical properties of a time series are invariant with respect to time reversal, we can say that this time series is reversal. Otherwise it is time irreversible. Till now, many indexes have been proposed to quantify the time series irreversibility of a complex system, such as multiscale time irreversibility [27–31], symbolic time series irreversibility [32], time irreversibility extracted from Poincaré plot [33–35], complex network time irreversibility [36, 37], and time irreversibility in high dimensional space [38, 39]. The scientific and engineering applications of time series irreversibility also involve many fields including financial system [40, 41], human heart rate [42–44], human brain [45], and seismicity [46]. Employing the time irreversibility index to analyze the two-phase flow fluctuating signals can effectively reveal the flow pattern formation, coalescence, and evolution characteristics. Also, the time irreversibility index can be an indicator for the flow pattern transition phenomenon, for example, from slug to bubble.

In this paper, we first carry out low flow rate oil-water two-phase flow experiment in vertical 20 mm inner diameter Plexiglass pipe and the conductance fluctuation time series which reflect the oil-in-water two-phase flow characteristics have been collected. Then we investigate the time irreversibility of the collected fluctuation series. Note that the dimension of an oil-water two-phase system is typically 5 or more [47]; we use Casali's multiple testing strategy [38] to detect the oil bubble flow time irreversibility. Multiscale analysis method has also been employed to the time irreversibility detection, considering that oil-water two-phase flow dynamics can be revealed more clearly under different scales [48–50]. Moreover, we propose a novel criterion, that is, average of multiscale time irreversibility (AMSI) to quantitatively characterize the two-phase flow system time irreversibility. The results suggest that AMSI can be a sensitive indication to predict the flow pattern transition phenomenon.

2. Experiments and Data Acquisition

2.1. Experimental Setup. We carried out the low flow rate oil-water two-phase flow experiment in a vertical 20 mm inner diameter Plexiglass pipe. As shown in Figure 1, the oil-water two-phase flow loop consists of a water tank, an oil tank, a mix tank, two peristaltic metering pumps, and testing pipes.

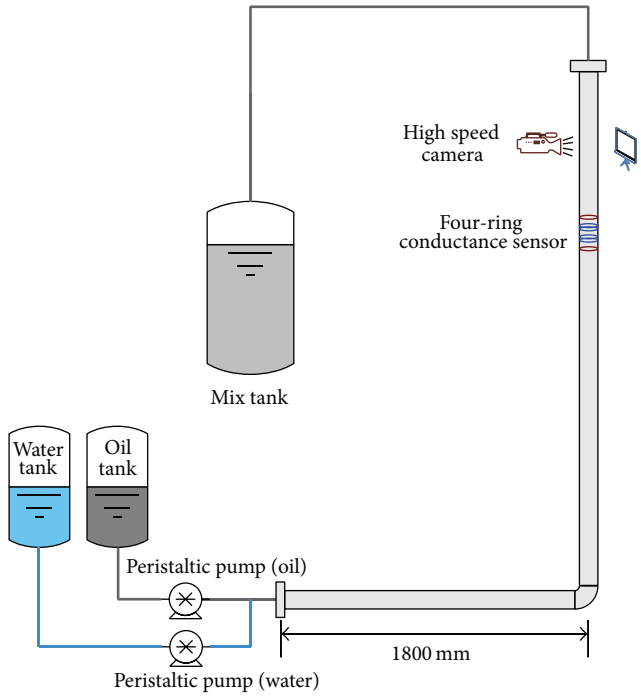

Figure 1: Schematic of oil-water flow loop facility.

During the experiment, the two phases, that is, oil and water, are first pumped out from the tanks, respectively, and mixed in the horizontal pipe section. Then the mixed fluid flows into the vertical test pipe, on which the measurement facility and sensor are installed. After the flow parameters and fluctuation measurement are done, the mixed fluid is drained into the mix tank to separate. The peristaltic pumps we used in the experiment are high precision metering pump, which can ensure precision of inlet flow rate and phase fraction.

In the experiment we employ a four-ring conductance sensor to collect the fluctuation signals. As shown in Figure 2, the sensor consists of four stainless steel pieces which are axially separated and flush mounted on the inside wall of the testing pipe. E1-E2 are the excitation electrodes that connected to a 20 KHz sinusoidal signal. H1-H2 are the measuring electrodes and the conductance fluctuating signals measured from H1-H2 are mainly correlated with the fluid fluctuations and dynamics. The detailed description of sensor geometry and working principle refers to our previous literatures [4, 51]. During the experiment, we also use a high speed digital camera to take snapshots of the fluid to identify the flow patterns and monitor the flow state.

The experimental schedule is as follows: we first fix the value of water phase fraction and then gradually increase the total velocity of the oil-water mixture flow. When the total flow rate reaches a preset value, the conductance fluctuation signal is collected. In the experiment, the water phase fraction is in the range of 70%–100%, while the mixture total flow rate was set at 0.01842 m/s, 0.03684 m/s, 0.07368 m/s, 0.11052 m/s, 0.14737 m/s, 0.18421 m/s, and 0.22105 m/s, respectively. The experiential mediums were tap water and white oil with a density of 856 kg/m^3 and a viscosity of 11.984 cP (40 1C).

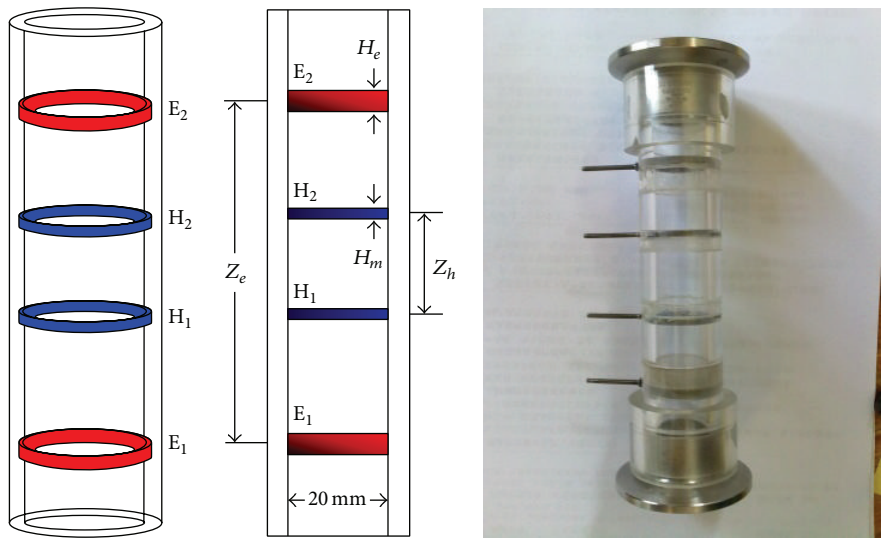

FIGURE 2: The four-ring conductance sensor. (a) Schematic of the sensor. (b) Real photo of the sensor.

The fluctuation signals from four-ring conductance sensor were recorded by National Instrument Corporation's data acquisition card PXI 4472 which operated by LabVIEW software. During the experiment, we set the sampling rate as 6000 and the sampling duration as 30 s.

2.2. Flow Patterns and the Collected Conductance Fluctuation Signals. In the experiment we observed three kinds of oil dispersed flow patterns, that is, oil slug flow, oil bubble flow, and the very fine dispersed oil bubble flow (VFD bubble flow). The collected typical conductance signals under different mixture velocity are shown in Figure 3. Oil slug flow is the flow pattern that often occurs in very low mixture velocity. In this situation, the dispersed oil phase coalesces into oil slugs. With the aid of high speed camera, we observed that the oil slugs intermittently pass through the vertical testing pipe, and the intervals between two slugs exhibit some disequilibrium. As shown in Figure 3, the conductance signals of oil slug flow show obvious intermittent fluctuations indicating the large oil slugs passing through the sensitive area of the sensor. We also observed that the slug fluctuation amplitude is much higher than that of the other two flow patterns.

With increasing the total mixture velocity, the flow pattern changes to oil bubble flow. From the snapshots taken by high speed camera we find that the oil phase of bubble flow is distributed in the continuous water phase in the form of discrete bubbles, and the random motions of oil bubbles resulting in the conductance fluctuation signals show stochastic character. With even more increasing of the total mixture velocity, the discrete oil bubbles change to very small oil droplets that are uniformly distributed in the continuous water phase which is known as VFD bubble flow. The fluctuation signals of this flow pattern are noise-like but with even lower fluctuation amplitude than that of oil bubble flow.

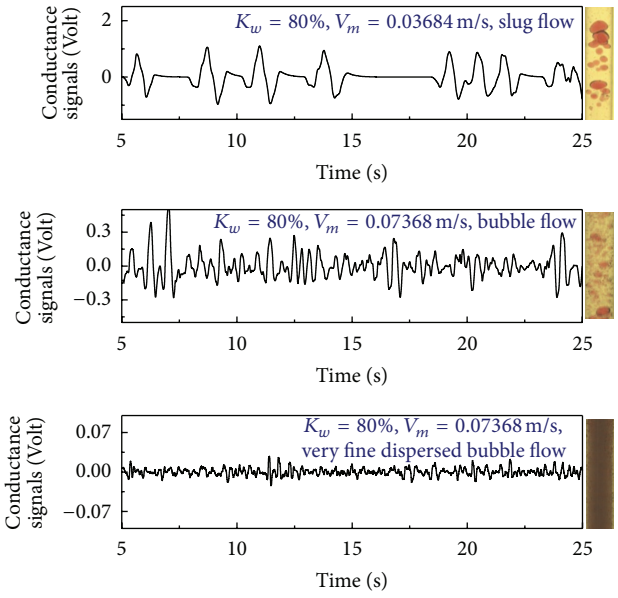

FIGURE 3: The conductance signals of three typical flow patterns.

3. Multiscale Time Irreversibility Index in m-Dimensional Phase Space

Note that the underlying flow dynamics of oil-in-water two-phase flow can be revealed more clearly and efficiently in multidimensional phase space; we employ Casali's multitesting strategy [38] to detect the m-dimensional time irreversibility of the oil-in-water two-phase flow. In addition, we extend this m-dimensional time irreversibility index with multiscale method, in the sense that oil-water two-phase flow exhibits various flow dynamics on different scales.

3.1. Multiple Testing Strategy for Irreversibility. Given a time series $x(i) = \{x_1, x_2, \ldots, x_n\}$, the reconstructed m-dimensional vector can be expressed as

$$X(t) = [x(t), x(t+\tau), \ldots, x(t+(m-1)\tau)], \quad (1)$$

where τ refers to the delay time and m refers to the embedded dimension. The irreversibility of a time series in the bidimensional space can be revealed by quantified distribution of data points in the bidimensional plane $(x(i), x(i+1))$ [33] or can be extracted by the probability characteristics of increments time series $y(t) = x(i+1) - x(i)$ [27]. In order to detect multidimensional time irreversibility of a complex system, Casali et al. [38] first project the reconstructed phase space on to any orthogonal two-dimensional plane $(x(i), x(i+L))$, where $L = 0, \ldots, m-1$; then the m-dimensional time irreversibility can be evaluated by analyzing data distribution in each two-dimensional plane.

Here we employ Costa's index [27] to detect the time irreversibility of each projected plane. First we map the projections in each plane into increment series:

$$y_L(i) = x(i+L) - x(i), \quad 1 < i \le n - m + 1, \quad (2)$$

where $y_L(i)$ refers to the increment series of plane $(x(i), x(i+L))$, and the time irreversibility index of this plane can be defined as follows:

$$A(L) = \frac{\sum_{y_L>0} P(y_L) \ln[P(y_L)] - \sum_{y_L>0} P(y_L) \ln[P(y_L)]}{\sum_{y_L} P(y_L) \ln[P(y_L)]}. \quad (3)$$

In (3) Shannon entropy is adopted to evaluate the system irreversibility, where $P(y_L)$ denotes the probability of the value y_L. Histogram of y_L is calculated to get the probability $P(y_L)$, and bin size is selected as the inverse of the signal sampling frequency. The number of data points in each bin and the bin number give the probability $P(y_L) = H(n)/N$, where $H(n)$ refers to the number of positive or negative data points in each bin and N refers to the divided bin number. $A(L)$ denotes the time irreversibility in plane $(x(i), x(i+L))$. The time irreversibility of an m-dimensional complex system then can be quantified by the following equation:

$$R = \frac{1}{m-1} \sum_{L=1}^{m-1} A(L). \quad (4)$$

The system irreversibility can be characterized by (4). If R equals 0, the system is reversible, and the more R deviate from 0 the more irreversible the system is.

3.2. Multiscale Time Series Irreversibility. Complex systems always exhibit various behaviors at different scales, so it is an effective way to characterize the system dynamics from multiscale prospective. In this paper we extend the multiple testing strategy [38] for irreversibility with multiscale method [27]. First, we map the original time series $x(i) = \{x_1, x_2, \ldots, x_n\}$ to coarse-grained time series as follows:

$$z^s(j) = \frac{1}{s} \sum_{i=(j-1)s+1}^{js} x(i), \quad 1 \le j \le \frac{n}{s}, \quad (5)$$

where $z^s(j)$ denotes the coarse-grained time series at scale s. Then by using $z^s(j)$, we can calculate the m-dimensional time irreversibility at each scale with (4):

$$R(s) = \frac{1}{m} \sum_{L=1}^{m-1} A_s(L), \quad (6)$$

where $R(s)$ refers to the m-dimensional time irreversibility at scale s and $A_s(L)$ denotes the time irreversibility index in projected plane $(x(i), x(i+L))$ at scale s. With this defined multiscale m-dimensional time irreversibility, we can detect the system disequilibrium in the multidimensional space which would provide rich dynamic information. In addition, adopting multiscale strategy provides a new way to reveal the system asymmetry from micro to the macro, which can characterize the complex system more precisely and clearly.

We now demonstrate how to quantitatively characterize the system disequilibrium with the average value of multiscale irreversibility (AMSI). This quantitative index can be expressed as follows:

$$\mathrm{AMSI} = \sum_{s=1}^{k} R(s), \quad (7)$$

where AMSI refers to the average value of multiscale irreversibility and the scale range is from 1 to k.

4. Time Irreversibility Dynamics of Oil-in-Water Two-Phase Flow

4.1. Multidimensional Phase Space of Dispersed Oil Bubble and Slug Fluctuating Signals. With the defined multiple time irreversibility testing strategy, we explore the disequilibrium and underlying dynamics of three typical flow patterns, that is, oil slug flow, oil bubble flow, and very fine dispersed oil bubble flow. According to the embedded theory and the previous study of oil-water two-phase flow at similar flow conditions [47], we here choose the embedded dimension $m = 5$ and delay time $\tau = 6$ ms. Figure 4 shows the return maps of three different oil-water two-phase flow patterns at each projected two-dimensional plane. In order to spread the attractor and get a clear view, in Figure 4, we use coarse-grained signals at scale 20 to reconstruct the phase space. As we can see, the return map of slug flow shows up as obvious evolution trajectory and the range of the data points is relatively wider than that of the other two flow patterns, indicating the large signal fluctuations caused by the existence of oil slugs. The data range of oil bubble flow decreases comparing to that of the oil slug flow, due to the lower signal fluctuating amplitude. Also, we find that there still exist trajectories in the return map, indicating the existence of large oil bubbles formed by the bubble coalescence. Data points of VFD oil bubble flow are uniformly distributed in even smaller range, which show the stationary and stochastic character of small dispersed oil droplets. In Figure 4, the return maps in different projection plane contain rich dynamic information. Detecting the flow pattern disequilibrium from different projected plan can provide a novel way to characterize the flow pattern dynamic and evolution characteristic.

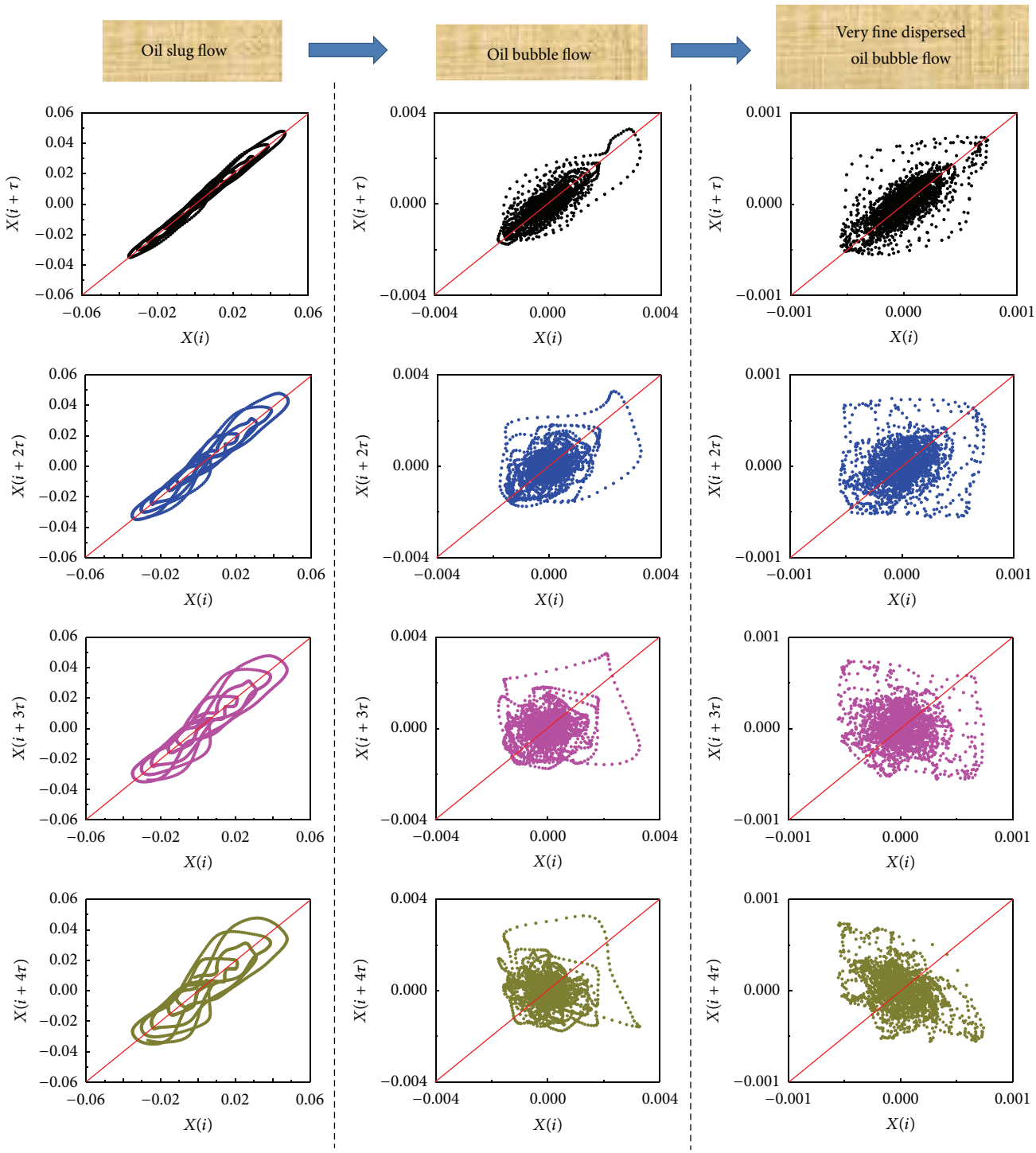

FIGURE 4: Return maps of three typical flow patterns at each projected two-dimensional plane. Each column represents the orthogonal projected planes of a typical flow pattern.

We also adopt the surrogate data approach [52, 53] to check the irreversibility of the collected fluctuation signals. Each of the 120 collected fluctuation signals has been used to generate surrogate data; thus a set of 120 surrogate types of data have been obtained. Figure 5 shows the return map of typical surrogate data and original signals for slug flow and bubble flow. We find that the original signals of oil slug flow demonstrate clear asymmetry while the surrogate data of slug flow shows symmetry. This indicated the irreversibility feature of oil slug flow. What is more, compared to that of slug flow, original signals of bubbly flow show less asymmetry in the sense of the uniform distribution of oil bubbles.

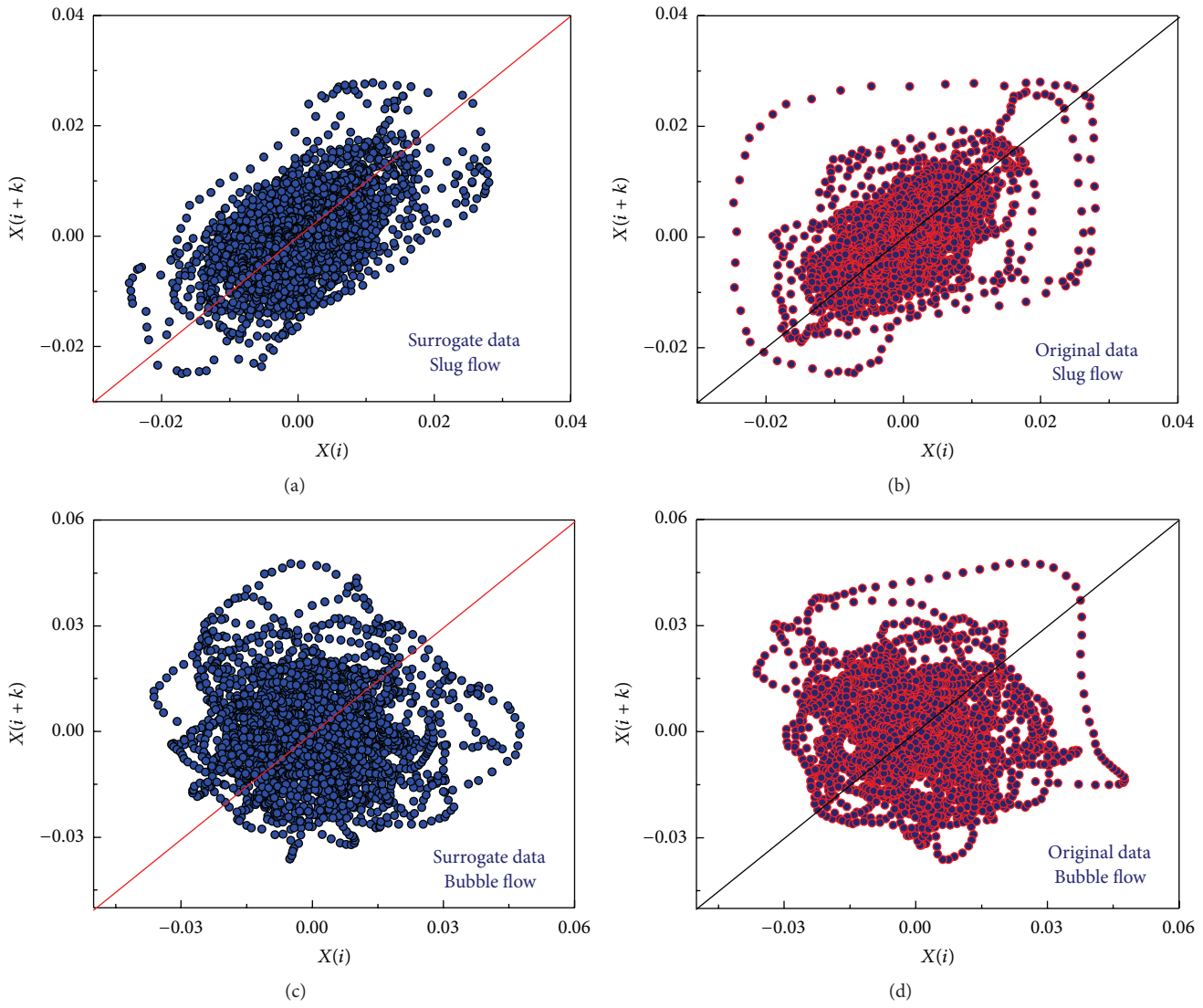

FIGURE 5: Return map of original signal and surrogate data. (a) Typical surrogate data of slug flow, (b) typical original signal of slug flow, (c) typical surrogate data of bubble flow, and (d) typical original signal of bubble flow.

The irreversibility index (AMSI) of original signals and surrogate signals is calculated and the results are shown in Figure 6, as we can see from original data irreversibility index, there exist obvious irreversibility changes when the flow pattern transition occurs (the flow pattern evolves from slug to bubble). However, the surrogate data irreversibility indexes of three different flow patterns are close to 0 and have no obvious changes, indicating that the nonlinear dynamics associate with flow pattern transition which is responsible for the data asymmetric distribution.

4.2. Detecting Oil-in-Water Two-Phase Flow Dynamics with Multiscale Time Irreversibility Index. Oil-water two-phase flow is quite a complex system such that the evolution of the flow pattern exhibits obvious polymorphism. In this regard, characterizing the flow pattern dynamics and irreversibility at a fixed time scale seems inadequate. Multiscale analysis method provides an effective way to investigate the system characteristics from macro to micro. Investigating the multiscale time irreversibility of typical flow pattern signals can not only reveal the flow pattern disequilibrium, but also detect the flow pattern evolution character such as the bubble coalescence and breakup. We calculate the multiscale time irreversibility index of oil-water two-phase flow fluctuating signals with (6) and the scale range is from 1 to 50. The length of original analyzed signals is 60000 points with the sampling frequency of 6000. At the scale of 50 the length of the coarse-grained signal is 1200 points which keeps a sufficient number to safely estimate the irreversibility index. As shown in Figure 7 we list the multiscale index of eight typical flow conditions at a fixed water-cut (84%) while increasing the mixed velocity (from 0.01842 m/s to 0.22105 m/s). Three typical flow patterns are observed, that is, oil slug flow, oil bubble flow, and VFD oil bubble flow. As we can see in

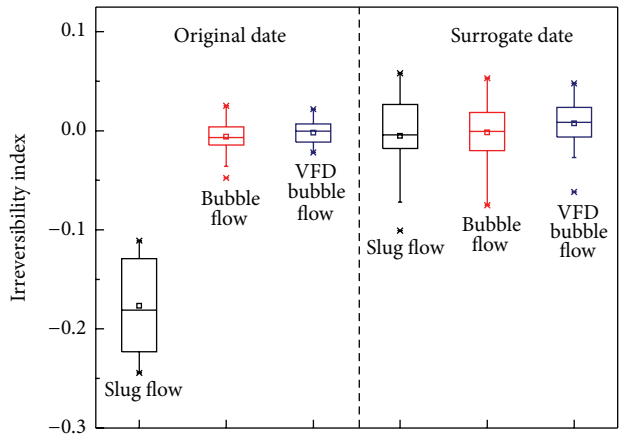

FIGURE 6: Time irreversibility index of original signals and the surrogate data.

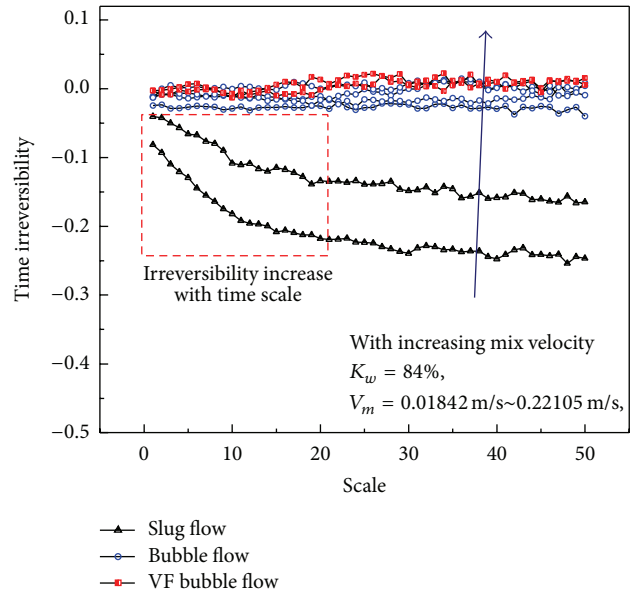

FIGURE 7: Multiscale time irreversibility of three typical flow patterns (water-cut K_w = 84% and mixture velocity V_m = 0.01842 m/s~0.22105 m/s).

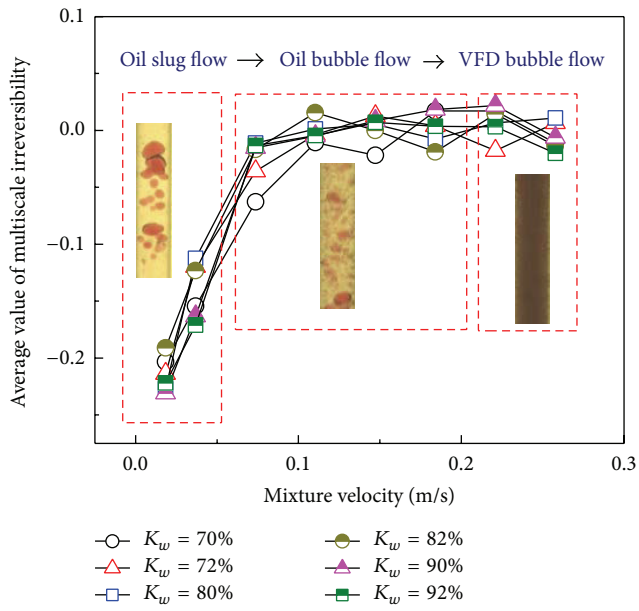

FIGURE 8: Average value of multiscale irreversibility under different mixture velocity.

Figure 7, the time irreversibility index of VFD bubble flow is around zero, which shows that the dispersed oil droplets are uniformly distributed in water and the mixed fluid is symmetrical. We also notice that the time irreversibility index has no obvious change from scale 1 to scale 50, indicating that the fluid structure of VFD bubble flow is symmetrical from micro to macro; that is, the mixed flow is spatially homogeneous along the pipe. Comparing to the VFD oil bubble flow, the time irreversibility of oil bubble flow has no obvious changes; the value of the irreversibility is still around 0 and independent of time scale. It reveals that although the mixture velocity of oil bubble flow decreases and the very fine dispersed oil droplets begin to coalesce into discrete oil bubbles, the oil bubbles still remain uniformly distributed and the flow structure shows spatially symmetrical character. It is also worth noticing that, under certain flow condition of low mixture velocity, the time irreversibility index of bubble flow slightly deviates from 0. This is probably due to the occasional presence of very large oil bubbles which are formed by the coalescence of discrete oil bubbles under low turbulence intensity. Oil slug flow occurs at very low mixture velocity; in this situation the flow turbulence intensity is extremely low and the dispersed oil phase coalesces into oil slug and bubble clusters. The intermittent presence of oil slugs in the pipe makes the fluid show disequilibrium and asymmetry feature. The multiscale time irreversibility index of slug flow has versified this phenomenon. As shown in Figure 7, the irreversibility index of oil slug flow is obvious which deviates from 0, showing the asymmetry character of slug flow. We also notice that the time irreversibility of slug flow increases with scale (the absolute value of irreversibility index increases with scale), indicating the disequilibrium and asymmetry of slug flow increase from micro special scale to macro special scale along the pipe.

We now demonstrate how to quantitatively characterize the flow disequilibrium under certain flow conditions with the average value of multiscale irreversibility (AMSI). Figure 8 shows the AMSI under different mixture velocity where the water-cut is fixed at 70%, 72%, 80%, 82%, 90%, and 92%, respectively. As shown in the figure, with increasing the mixture velocity, the flow pattern evolves from oil slug flow to oil bubble flow and then VFD oil bubble flow. Correspondingly, the AMSI gradually increases. That is, the asymmetry of the mixed fluid decreases with increasing the mixture flow rate (the more the time irreversibility index deviated from 0, the more the asymmetry of the mixed fluid is). This can also be interpreted by the flow pattern evolution characteristics. Oil slug flow occurs at very low mixture velocity and the dispersed oil phase coalesces into large intermittent oil slugs, which lead to asymmetric

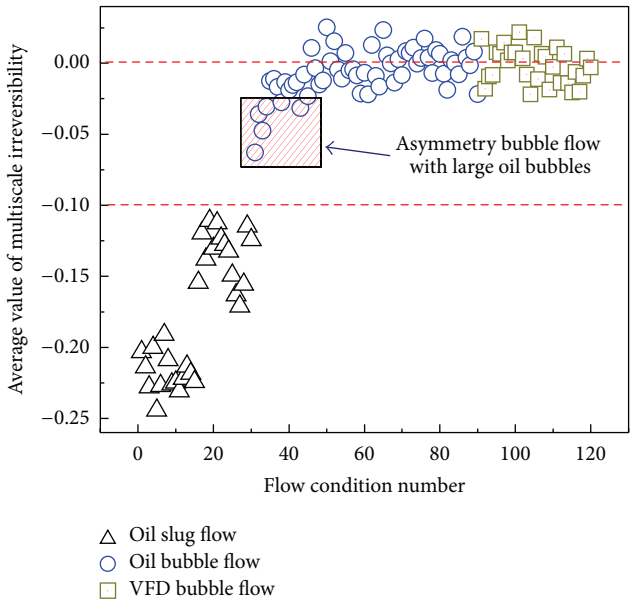

Figure 9: The average value of multiscale irreversibility of all the flow conditions.

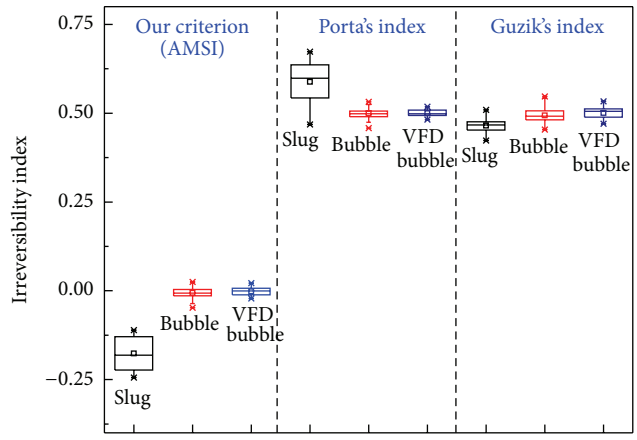

Figure 10: Comparison of AMSI index, Porta's index [33], and Guzik's index [34].

character of the fluid structure. With increasing the mixture velocity, the turbulent intensity is high enough to break up the oil slugs into uniformly distributed oil bubbles and flow pattern changes to oil bubble flow. In this situation the flow structure changes from asymmetric to symmetric and the time irreversibility index is around 0. With even more increasing the mixture velocity, discrete oil bubbles are broken into smaller oil droplets which are also uniformly distributed. In this regard, the flow structure shows symmetry and the time irreversibility index is also around 0.

Figure 9 shows the AMSI of all 120 flow conditions. As we can see, most AMSI indexes of bubble flow and VFD bubble flow are around 0, indicating that oil bubble flow and VFD oil bubble flow are basically symmetric. Also, it is worth noticing that some AMSI indexes of oil bubble flow slightly derived from 0, which is probably because of the occasional presence of large oil bubbles that change the symmetry of the mixed fluid. The AMSI index of oil slug flow is lower than that of the other two flow patterns, and it is obviously deviated from 0 (below −0.1), which shows the asymmetrical character of the intermittent oil slugs. From this point of view the AMSI index can not only be used to characterize the two-phase flow spatial asymmetry and detect the flow pattern dynamic but also be employed as a criterion to identify the pattern transition and bubble coalescence.

We also compared the proposed AMSI index with other two time irreversibility indexes, that is, Porta's index [33] and Guzik's index [34]. As shown in Figure 10, both the AMSI index and Porta's index [33] can effectively demonstrate the system irreversibility when the flow pattern transition occurs (both the AMSI index and Porta's index [33] have obvious changes with the flow pattern evolving from slug to bubble flow). However, Guzik's index [34] is less sensitive for characterizing the flow pattern transition dynamics. So we think that the proposed AMSI index is sufficient and effective for characterizing the dynamics associated with the flow pattern transition.

5. Conclusions

Characterizing the low flow rate oil-in-water two-phase flow disequilibrium with experimental measurement signals has been a challenging problem in the fields of time series analysis and fluid dynamics. In this paper, we first experimentally investigate the oil-in-water two-phase flow in a vertical pipe and collect conductance fluctuating time series that reflect the fluid dynamics. Then we detected the flow disequilibrium with two strategies, that is, multidimensional time irreversibility and multiscale time irreversibility. We find that the collected fluctuating signals of oil bubble flow and very fine dispersed oil bubble flow are reversible while the signals of slug flow show irreversible character. This indicates that both the oil bubble flow and very fine dispersed oil bubble flow have the symmetric structure while oil slug flow shows asymmetric flow characteristics due to the intermittent presence of oil slugs. Moreover, we propose a novel criterion, that is, AMSI, to quantitatively characterize the flow asymmetry character. The results show that the AMSI which is sensitive to the flow conditions can be used to identify flow patterns and predict dispersed phase coalescence phenomenon. Our research not only reveals the oil-water two-phase flow pattern evolution character but also provides a novel application of time series irreversibility analysis to uncover the fluid dynamics.

Competing Interests

The authors declare that they have no competing interests.

Acknowledgments

This work was supported by National Natural Science Foundation of China (Grant no. 61301246) and Tianjin Higher Educational Science and Technology Program (Grant no. 20140710).

References

[1] G. W. Govier, G. A. Sullivan, and R. K. Wood, "The upward vertical flow of oil-water mixtures," *The Canadian Journal of Chemical Engineering*, vol. 39, no. 2, pp. 67–75, 1961.

[2] J. G. Flores, X. T. Chen, C. Sarica, and J. P. Brill, "Characterization of oil-water flow patterns in vertical and deviated wells," in *Proceedings of the SPE Annual Technical Conference and Exhibition*, San Antonio, Tex, USA, October 1997.

[3] A. K. Jana, G. Das, and P. K. Das, "Flow regime identification of two-phase liquid-liquid upflow through vertical pipe," *Chemical Engineering Science*, vol. 61, no. 5, pp. 1500–1515, 2006.

[4] M. Du, N.-D. Jin, Z.-K. Gao, Z.-Y. Wang, and L.-S. Zhai, "Flow pattern and water holdup measurements of vertical upward oil-water two-phase flow in small diameter pipes," *International Journal of Multiphase Flow*, vol. 41, pp. 91–105, 2012.

[5] M. Pietrzak, "Flow patterns and volume fractions of phases during liquid-liquid two-phase flow in pipe bends," *Experimental Thermal and Fluid Science*, vol. 54, pp. 247–258, 2014.

[6] D. Tsaoulidis, V. Dore, P. Angeli, N. V. Plechkova, and K. R. Seddon, "Flow patterns and pressure drop of ionic liquid-water two-phase flows in microchannels," *International Journal of Multiphase Flow*, vol. 54, pp. 1–10, 2013.

[7] D. Picchi, D. Strazza, M. Demori, V. Ferrari, and P. Poesio, "An experimental investigation and two-fluid model validation for dilute viscous oil in water dispersed pipe flow," *Experimental Thermal and Fluid Science*, vol. 60, pp. 28–34, 2015.

[8] G. P. Lucas and X. Zhao, "Large probe arrays for measuring mean and time dependent local oil volume fraction and local oil velocity component distributions in inclined oil-in-water flows," *Flow Measurement and Instrumentation*, vol. 32, pp. 76–83, 2013.

[9] K. Mydlarz-Gabryk, M. Pietrzak, and L. Troniewski, "Study on oil-water two-phase upflow in vertical pipes," *Journal of Petroleum Science and Engineering*, vol. 117, pp. 28–36, 2014.

[10] J. Zhang, J.-Y. Xu, Y.-X. Wu, D.-H. Li, and H. Li, "Experimental validation of the calculation of phase holdup for an oil-water two-phase vertical flow based on the measurement of pressure drops," *Flow Measurement and Instrumentation*, vol. 31, pp. 96–101, 2013.

[11] H. Zhou, L. Xu, Z. Cao, J. Hu, and X. Liu, "Image reconstruction for invasive ERT in vertical oil well logging," *Chinese Journal of Chemical Engineering*, vol. 20, no. 2, pp. 319–328, 2012.

[12] W. Wang, Y. Zheng, Z. Li, and K. Lee, "PIV investigation of oil–mineral interaction for an oil spill application," *Chemical Engineering Journal*, vol. 170, no. 1, pp. 241–249, 2011.

[13] J. Zhang and M. Small, "Complex network from pseudoperiodic time series: topology versus dynamics," *Physical Review Letters*, vol. 96, Article ID 238701, 2006.

[14] R. V. Donner, M. Small, J. F. Donges et al., "Recurrence-based time series analysis by means of complex network methods," *International Journal of Bifurcation and Chaos in Applied Sciences and Engineering*, vol. 21, no. 4, pp. 1019–1046, 2011.

[15] H.-W. Li, Y.-L. Zhou, Y.-D. Hou, B. Sun, and Y. Yang, "Flow pattern map and time-frequency spectrum characteristics of nitrogen-water two-phase flow in small vertical upward non-circular channels," *Experimental Thermal and Fluid Science*, vol. 54, pp. 47–60, 2014.

[16] D. P. Chakrabarti, G. Das, and P. K. Das, "The transition from water continuous to oil continuous flow pattern," *AIChE Journal*, vol. 52, no. 11, pp. 3668–3678, 2006.

[17] H. Ding, Z. Huang, Z. Song, and Y. Yan, "Hilbert-Huang transform based signal analysis for the characterization of gas–liquid two-phase flow," *Flow Measurement and Instrumentation*, vol. 18, no. 1, pp. 37–46, 2007.

[18] Z. Y. Wang, N. D. Jin, Z. K. Gao, Y. B. Zong, and T. Wang, "Nonlinear dynamical analysis of large diameter vertical upward oil-gas-water three-phase flow pattern characteristics," *Chemical Engineering Science*, vol. 65, no. 18, pp. 5226–5236, 2010.

[19] H. O. Ghaffari and R. P. Young, "Network configurations of dynamic friction patterns," *Europhysics Letters*, vol. 98, no. 4, Article ID 48003, 2012.

[20] H. O. Ghaffari, M. Sharifzadeh, and R. P. Young, "Complex aperture networks," *Physica A: Statistical Mechanics and its Applications*, vol. 392, no. 4, pp. 1028–1037, 2013.

[21] H. O. Ghaffari and R. P. Young, "Acoustic-friction networks and the evolution of precursor rupture fronts in laboratory earthquakes," *Scientific Reports*, vol. 3, article 1799, 2013.

[22] Z. K. Gao, Y. X. Yang, P. C. Fang, N. D. Jin, C. Y. Xia, and L. D. Hu, "Multi-frequency complex network from time series for uncovering oil-water flow structure," *Scientific Reports*, vol. 5, article 8222, 2015.

[23] Z.-K. Gao, P.-C. Fang, M.-S. Ding, and N.-D. Jin, "Multivariate weighted complex network analysis for characterizing nonlinear dynamic behavior in two-phase flow," *Experimental Thermal and Fluid Science*, vol. 60, pp. 157–164, 2015.

[24] Z.-K. Gao and N.-D. Jin, "A directed weighted complex network for characterizing chaotic dynamics from time series," *Nonlinear Analysis: Real World Applications*, vol. 13, no. 2, pp. 947–952, 2012.

[25] Z.-K. Gao, W.-X. Zhang, D.-N. Jin, R. V. Donner, N. Marwan, and J. Kurths, "Recurrence networks from multivariate signals for uncovering dynamic transitions of horizontal oil-water stratified flows," *Europhysics Letters*, vol. 103, no. 5, Article ID 50004, 2013.

[26] Z.-K. Gao, X.-W. Zhang, N.-D. Jin, N. Marwan, and J. Kurths, "Multivariate recurrence network analysis for characterizing horizontal oil-water two-phase flow," *Physical Review E-Statistical, Nonlinear, and Soft Matter Physics*, vol. 88, no. 3, Article ID 032910, 2013.

[27] M. Costa, A. L. Goldberger, and C.-K. Peng, "Broken asymmetry of the human heartbeat: loss of time irreversibility in aging and disease," *Physical Review Letters*, vol. 95, no. 19, Article ID 198102, 2005.

[28] A. Porporato, J. R. Rigby, and E. Daly, "Irreversibility and fluctuation theorem in stationary time series," *Physical Review Letters*, vol. 98, no. 9, Article ID 094101, 2007.

[29] M. D. Costa, C.-K. Peng, and A. L. Goldberger, "Multiscale analysis of heart rate dynamics: entropy and time irreversibility measures," *Cardiovascular Engineering*, vol. 8, no. 2, pp. 88–93, 2008.

[30] J. Xia, P. Shang, J. Wang, and W. Shi, "Classifying of financial time series based on multiscale entropy and multiscale time irreversibility," *Physica A: Statistical Mechanics and Its Applications*, vol. 400, pp. 151–158, 2014.

[31] B. Czippelova, L. Chladekova, Z. Uhrikova, K. Javorka, M. Zibolen, and M. Javorka, "Time irreversibility of heart rate oscillations in newborns—does it reflect system nonlinearity?" *Biomedical Signal Processing and Control*, vol. 19, pp. 85–88, 2015.

[32] C. Cammarota and E. Rogora, "Time reversal, symbolic series and irreversibility of human heartbeat," *Chaos, Solitons & Fractals*, vol. 32, no. 5, pp. 1649–1654, 2007.

[33] A. Porta, S. Guzzetti, N. Montano, T. Gnecchi-Ruscone, R. Furlan, and A. Malliani, "Time reversibility in short-term heart period variability," *Computing in Cardiology*, vol. 33, pp. 77–80, 2006.

[34] P. Guzik, J. Piskorski, T. Krauze, A. Wykretowicz, and H. Wysocki, "Heart rate asymmetry by Poincaré plots of RR intervals," *Biomedizinische Technik*, vol. 51, no. 4, pp. 272–275, 2006.

[35] C. Huo, X. Huang, J. Zhuang, F. Hou, H. Ni, and X. Ning, "Quadrantal multi-scale distribution entropy analysis of heartbeat interval series based on a modified poincaré plot," *Physica A: Statistical Mechanics and Its Applications*, vol. 392, no. 17, pp. 3601–3609, 2013.

[36] L. Lacasa, A. Nuñez, E. Roldán, J. M. R. Parrondo, and B. Luque, "Time series irreversibility: a visibility graph approach," *The European Physical Journal B*, vol. 85, article 217, 2012.

[37] J. F. Donges, R. V. Donner, and K. Jürgen, "Testing time series irreversibility using complex network methods," *Europhysics Letters*, vol. 102, no. 1, Article ID 10004, 2013.

[38] K. R. Casali, A. G. Casali, N. Montano et al., "Multiple testing strategy for the detection of temporal irreversibility in stationary time series," *Physical Review E*, vol. 77, no. 6, Article ID 066204, 2008.

[39] F. Z. Hou, X. B. Ning, J. J. Zhuang, X. L. Huang, M. J. Fu, and C. H. Bian, "High-dimensional time irreversibility analysis of human interbeat intervals," *Medical Engineering & Physics*, vol. 33, no. 5, pp. 633–637, 2011.

[40] Y.-T. Chen and C.-M. Kuan, "Time irreversibility and egarch effects in US stock index returns," *Journal of Applied Econometrics*, vol. 17, no. 5, pp. 565–578, 2002.

[41] P. Wild, J. Foster, and M. J. Hinich, "Testing for non-linear and time irreversible probabilistic structure in high frequency financial time series data," *Journal of the Royal Statistical Society. Series A: Statistics in Society*, vol. 177, no. 3, pp. 643–659, 2014.

[42] F. Hou, J. Zhuang, C. Bian et al., "Analysis of heartbeat asymmetry based on multi-scale time irreversibility test," *Physica A: Statistical Mechanics and Its Applications*, vol. 389, no. 4, pp. 754–760, 2010.

[43] J. Piskorski and P. Guzik, "Asymmetric properties of long-term and total heart rate variability," *Medical and Biological Engineering and Computing*, vol. 49, no. 11, pp. 1289–1297, 2011.

[44] B. D. L. C. Torres and J. N. Orellana, "Multiscale time irreversibility of heartbeat at rest and during aerobic exercise," *Cardiovascular Engineering*, vol. 10, no. 1, pp. 1–4, 2010.

[45] M. Zhang and J. Wang, "Modified symbolic relative entropy based electroencephalogram time irreversibility analysis," *Acta Physica Sinica*, vol. 62, no. 3, Article ID 038701, 2013.

[46] L. Telesca and M. Lovallo, "Analysis of seismic sequences by using the method of visibility graph," *Europhysics Letters*, vol. 97, no. 5, Article ID 50002, 2012.

[47] G. M. Oddie, "On the detection of a low-dimensional attractor in disperse two-component (oil-water) flow in a vertical pipe," *Flow Measurement and Instrumentation*, vol. 2, no. 4, pp. 225–231, 1991.

[48] Y. B. Zong and N. D. Jin, "Multi-scale recurrence plot analysis of inclined oil-water two phase flow structure based on conductance fluctuation signals," *European Physical Journal: Special Topics*, vol. 164, no. 1, pp. 165–177, 2008.

[49] G.-B. Zheng and N.-D. Jin, "Multiscal entropy and dynamic characteristics of two phase flow patterns," *Acta Physica Sinica*, vol. 58, no. 7, pp. 4485–4492, 2009.

[50] M. Du, N.-D. Jin, Z.-K. Gao, L. Zhu, and Z.-Y. Wang, "Multiscale permutation entropy analysis of oil-in-water type two-phase flow pattern," *Acta Physica Sinica*, vol. 61, no. 23, Article ID 230507, 2012.

[51] N. D. Jin, Z. Xin, J. Wang, Z. Y. Wang, X. H. Jia, and W. P. Chen, "Design and geometry optimization of a conductivity probe with a vertical multiple electrode array for measuring volume fraction and axial velocity of two-phase flow," *Measurement Science & Technology*, vol. 19, no. 4, Article ID 045403, 2008.

[52] T. Schreiber and A. Schmitz, "Improved surrogate data for nonlinearity tests," *Physical Review Letters*, vol. 77, no. 4, pp. 635–638, 1996.

[53] A. Porta, K. R. Casali, A. G. Casali et al., "Temporal asymmetries of short-term heart period variability are linked to autonomic regulation," *American Journal of Physiology—Regulatory Integrative and Comparative Physiology*, vol. 295, no. 2, pp. R550–R557, 2008.